JOURNAL OF SOLID STATE CHEMISTRY 76, 64–86 (1988)

X-Ray Study of Transition-Metal Dopants in β-Boron*

G. A. SLACK, C. I. HEJNA, M. GARBAUSKAS, AND J. S. KASPER

General Electric Corporate Research and Development, Schenectady, New York 12301

Received November 9, 1987; in revised form March 11, 1988

The atomic locations and concentrations of various transition element dopants in single crystals of β-boron have been studied by X-ray methods. The elements include Sc, Ti, V, Cr, Mn, Fe, Co, Ni, Cu, Zr, Nb, Hf, and Ta. These dopants do not enter normal boron positions in the framework at the concentrations studied; rather they occupy previously identified A_1, A_2, D, or E sites. The percentage occupancies of the several sites are correlated with the atomic sizes of the dopant atoms and their concentrations. Some differences between samples are related to their thermal histories. A number of competing interactions between six different, partially occupied boron sites and the dopant sites have been found. The doping mechanism is "displacive" rather than interstitial or substitutional. © 1988 Academic Press, Inc.

I. Introduction

Numerous studies have reported the occurrence of various transition metals in β-boron. Single-crystal X-ray work has revealed which sites are actually occupied. The site nomenclature and positions are given by Andersson and Lundström (*3*). To date, there have been reports for Sc (*1*), V (*2*), Cr (*3*), Mn (*4*), Fe (*5*), Ni (*6*), Cu (*4, 7, 8*), and Zr (*9*). The nontransition elements Al (*10*), Si (*11*), and Ge (*12*) have also been studied. Some dopants also replace boron atoms as well as enter various interstitial sites. These dopants are known to expand the lattice (*13, 4*), increase the microhardness (*13*), and alter the electrical properties (*15–19*) of the host β-boron structure. These effects can be very complex as a function of dopant concentration because there are several possible dopant sites, and the site occupancy of a particular dopant may change with its concentration (*2, 8*). We report here on the site occupation for Sc, Ti, V, Cr, Mn, Fe, Co, Ni, Cu, Zr, Nb, Hf, and Ta as dopants in β-rhombohedral boron.

II. Crystal Growth

The crystal-growth techniques used are the same as those reported earlier in our work on V (*2*). The samples were all single crystals of β-boron grown from the melt using high-purity starting materials. The doped boron was melted in CVD boron nitride crucibles, and the crystals were grown by cooling the melt using either a fast-cooling (F) technique or a slow-cooling (S) technique (see Tables Ia, Ib, and II). The residual nitrogen concentration from the partial

* This work was supported in part by the U.S. Department of Energy on Contract DE-AC01-81NE32084.

0022-4596/88 $3.00

TABLE Ia

LATTICE PARAMETERS[a] AND OTHER DATA FOR SINGLE-CRYSTAL SAMPLES STUDIED

Dopant	Sample No.	a_o (Å)	c_o (Å)	V (Å^3)	R (%)	r (%)	No. reflections
Sc	180	10.916(6)	23.864(36)	2462.5(42)	5.1	4.1	679
Sc	192	10.953(1)	23.946(5)	2487.8(7)	4.7	3.7	1062
Ti	106	10.925(3)	23.913(11)	2471.8(24)	4.8	3.3	506
V	66	10.949(3)	23.840(10)	2475.1(24)	4.2	2.9	543
V	91	10.972(3)	23.908(9)	2492.6(23)	4.1	3.2	858
Cr	65	10.980(2)	23.882(3)	2493.5(13)	4.7	3.0	1115
Cr	115	10.983(2)	23.908(11)	2497.6(20)	3.1	5.7	707
Cr	93	10.993(3)	23.882(18)	2499.3(32)	8.3	8.3	699
Mn	67	10.959(3)	23.901(12)	2486.0(26)	4.7	2.4	675
Fe	64	10.955(2)	23.837(11)	2477.4(20)	7.4	8.4	704
Co	103	10.957(3)	23.840(9)	2478.7(23)	5.4	3.8	850
Ni	135	10.950(3)	23.851(10)	2476.5(22)	4.8	4.8	692
Ni	71	10.955(8)	23.865(22)	2480.4(37)	5.6	3.2	782
Ni	100	10.972(6)	23.839(20)	2485.4(33)	4.1	3.8	856
Cu	130	10.959(3)	23.874(10)	2483.1(25)	4.9	4.3	535
Cu	185	10.943(3)	23.885(6)	2476.9(18)	4.2	3.8	702
Zr	37	10.932(4)	23.849(11)	2468.3(26)	4.9	3.4	712
Nb	162	10.938(2)	23.858(10)	2472.0(20)	5.8	5.4	716
Hf	174	10.948(2)	23.909(11)	2481.8(20)	7.9	6.7	734
Hf	169	10.975(3)	24.034(5)	2507.1(19)	4.2	7.2	744
Ta	170	10.942(2)	23.898(4)	2477.8(14)	4.4	6.0	720
Pure boron	57	10.955(3)	23.855(6)	2479.3(20)	4.4	3.2	674
Pure boron	EP	10.937(3)	23.821(6)	2467.8(22)	4.1	2.1	1775

[a] a_o and c_o as measured by the Nicolet diffractometer.

dissolution of the crucible was measured for several crystals and was in the range 30 to 200 atomic ppm. For the F samples the melt was cooled at a rate of about 350°C/min, while for the S samples the cooling rate was about 2.2°C/min. The small single crystals used for the X-ray studies were obtained from the polycrystalline, solidified melt either by mechanical shattering or by slowly etching it with a hot mixture of HF + HNO_3 + H_2SO_4 acids until the residual pieces were a fraction of a millimeter in diameter. Often but not always, these small pieces were single crystals as determined by the X-ray diffraction pattern.

TABLE Ib

LATTICE PARAMETERS DETERMINED WITH GUINIER (Gu) OR GANDOLFI (Ga) CAMERA

	Camera	a_o (Å)	c_o (Å)	V (Å^3)	S
V66	Ga	10.9357(26)	23.7995(56)	2464.9(18)	+16(5)
V91	Ga	10.9311(81)	23.9459(177)	2477.9(55)	−50(15)
Cr65	Ga	10.9402(39)	23.8286(84)	2469.9(26)	+8(7)
Cr65	Gu	10.9377(23)	23.8255(51)	2468.5(16)	+7(4)
Cr115	Ga	10.9602(14)	23.8384(31)	2480.0(10)	+22(3)
Cr93	Gu	10.9696(21)	23.8400(46)	2484.4(14)	+30(4)
Zr37	Gu	10.9427(15)	23.9767(33)	2486.4(10)	−52(3)
Nb162	Gu	10.9251(18)	23.8283(38)	2463.0(12)	−6(3)
Ta170	Gu	10.9255(17)	23.8509(37)	2465.6(11)	−15(3)
Pure 57	Gu	10.9300(13)	23.8145(27)	2463.8(9)	+4(2)
Pure EP	Gu	10.9311(12)	23.8233(25)	2465.2(8)	+2(2)

III. X-Ray Investigation

The structural studies were made on single crystals 0.1 to 0.3 mm in diameter. The

TABLE II

CONTENTS OF THE HEXAGONAL UNIT CELL OF PURE AND DOPED β-BORON SAMPLES

Sample No.	Cooling rate	Atom% dopant		No. Atoms/ unit cell	
		Melt	X-ray data	Dopant	Boron
Sc180	S	0.99	1.24(3)	3.95(8)	315.6(11)
Sc192	S	1.96	1.54(2)	4.88(5)	311.9(3)
Ti106	S	1.96	1.90(2)	5.99(8)	309.9(5)
V66	F	0.99	0.60(9)	1.90(33)	316.4(10)
V91	S	1.96	1.57(4)	5.02(11)	314.4(11)
Cr65	F	0.99	1.04(1)	3.31(2)	315.0(8)
Cr115	S	1.48	1.43(1)	4.57(2)	314.7(6)
Cr93	F	1.96	1.48(4)	4.65(14)	310.0(3)
Mn67	F	0.99	0.73(2)	2.35(5)	317.6(9)
Fe64	F	0.99	1.12(3)	3.57(8)	316.1(10)
Co103	S	1.48	1.52(2)	4.80(5)	312.6(10)
Ni135	S	0.99	0.73(2)	2.33(5)	318.8(9)
Ni71	F	0.99	0.88(3)	2.84(9)	318.4(6)
Ni100	S	1.96	1.64(6)	5.32(16)	318.1(8)
Cu130	S	0.25	0.26(7)	0.83(22)	320.0(11)
Cu185	S	0.74	0.77(2)	2.48(5)	319.6(7)
Zr37	F	0.99	0.69(1)	2.20(4)	314.7(5)
Nb162	S	0.74	0.50(1)	1.58(3)	316.5(11)
Hf174	S	0.50	0.41(1)	1.31(2)	314.3(5)
Hf169	S	1.96	1.96(3)	6.22(6)	310.2(8)
Ta170	S	1.23	1.03(1)	3.25(2)	312.5(8)
Pure 57	F	0.00	0.00	0.00	319.1(13)
Pure EP	?	0.00	0.00	0.00	320.6(7)

X-ray diffraction intensities were measured on an automated four-circle diffractometer (Nicolet P3F, Nicolet Instrument Corp., Madison, WI) using monochromated molybdenum $K\alpha$ radiation (0.71069 Å). The structure was refined using the SHELXTL program package by Sheldrick[1] using the number of unique observed reflections listed in Table Ia. The intensities of some of the diffraction lines turn out to be quite sensitive to the presence of small amounts of transition metals in the boron structure and have permitted us to study metal concentrations as low as 0.25 atom%. No corrections were needed for absorption or extinction because of the low atomic mass and small crystal sizes used.

The space group is $R\bar{3}m$ in all cases, as it is in undoped β-rhombohedral boron (*20–23*). The lattice parameters for the hexagonal cell as measured with the single-crystal diffractometer are given in Table Ia. Some samples were powdered and lattice parameters were measured with a Huber–Guinier camera or a Gandolfi camera with greater precision. These are listed in Table Ib. Table Ia also gives the R factor resulting from the structure refinement. This R factor is defined as:

$$R = \frac{\Sigma[|F_o| - |F_c|]}{\Sigma |F_o|}. \qquad (1)$$

Here F_o and F_c are the observed and calculated scattering factors, with F_c taken from a standard reference (*24*). In all cases, F_c values are for the neutral atoms. The residual electron density, r, in Table Ia is expressed as a percentage of a boron peak for the highest remaining electron density found from a difference Fourier map. We have looked at the electron density in all of the eight interstitial sites identified by Andersson and Lundström (*3*) as well as the new boron sites found by Slack *et al.* (*23* . The results are given in Tables II, IIIa, and IIIb.

The x_o/a_o, y_o/a_o, z_o/c_o coordinates, the thermal parameters, and the percentage occupancies, P, for the occupied sites in the various samples are given in the Appendix.[2] From these, the interatomic distances have been calculated. For most of the boron atoms in the β-boron framework of our samples the boron–boron distances do not vary by more than ±0.04 Å from those in pure β-boron (*21, 23*). However the boron sites with low occupancy, B17, B18, B19, and B20, show considerable perturbation (see Tables IVa and IVb).

[1] G. M. Sheldrick, 1983, University of Göttingen, Federal Republic of Germany, distributed through Nicolet Instrument Corp.

[2] See NAPS Document No. 04602 for 24 pages of supplementary materials from ASIS/NAPS, Microfiche Publications, P.O. Box 3513, Grand Central Station, New York, NY 10163. Remit in advance $4.00 for microfiche copy or for photocopy, $7.75 up to 20 pages plus $.30 for each additional page. All orders must be prepaid.

TABLE IIIa

PERCENTAGE OCCUPANCY, *P*, OF PARTIALLY OCCUPIED BORON SITES IN β-BORON

Sample No.	B13 18h	B17 18h	B17d 36i	B18 18h	Σ_1[a]	B16 18h
Sc180	74.2(13)	11.3(19)	0.0	9.6(16)	95(5)	8.4(12)
Sc192	75.3(8)	0.0	0.0	0.0	75(1)	7.2(8)
Ti106	66.5(4)	0.0	0.0	0.0	66(1)	5.4(14)
V66	72.6(12)	9.3(14)	0.0	10.8(14)	93(4)	15.1(13)
V91	70.8(15)	0.0	5.6(13)	14.8(22)	97(6)	0.0
Cr65	71.9(11)	0.0	6.5(6)	9.3(10)	94(3)	5.8(10)
Cr115	69.8(11)	0.0	6.1(6)	16.5(11)	99(3)	0.0
Cr93	72.1(18)	0.0	0.0	0.0	72(2)	0.0
Mn67	69.8(12)	11.7(15)	0.0	10.3(14)	92(4)	23.5(12)
Fe64	75.3(12)	0.0	3.5(8)	10.3(17)	93(4)	13.6(13)
Co103	64.1(13)	1.8(14)	0.0	3.4(14)	69(4)	17.1(14)
Ni135	67.8(12)	14.3(16)	0.0	12.3(12)	94(4)	26.5(11)
Ni71	69.1(8)	0.0	6.4(5)	13.9(8)	96(3)	23.2(7)
Ni100	68.3(9)	0.0	7.3(7)	16.2(10)	99(3)	18.1(10)
Cu130	74.5(13)	0.0	6.1(11)	14.6(15)	102(5)	26.2(14)
Cu185	69.5(8)	0.0	6.8(6)	14.5(11)	98(3)	27.9(9)
Zr37	62.5(12)	0.0	0.0	0.0	63(1)	35.8(18)
Nb162	67.4(13)	0.0	5.1(8)	10.1(18)	88(5)	20.9(13)
Hf174	76.7(18)	0.0	0.0	0.0	77(2)	19.6(12)
Hf169	65.5(23)	0.0	0.0	0.0	66(2)	8.1(21)
Ta170	66.3(15)	0.0	2.5(10)	0.0	71(3)	14.7(14)
Pure 57	77.7(14)	0.0	3.2(8)	5.8(15)	97(7)	25.8(13)
Pure EP	74.5(6)	8.5(9)	0.0	6.6(6)	96(3)	27.2(7)

[a] Includes B19 and B20 occupancies for Pure 57 and Pure EP.

TABLE IIIb

PERCENTAGE OCCUPANCY, *P*, FOR DOPANT SITES IN β-BORON

Sample No.	A_1 6c	D 18h	Dd 36i	E 6c	Σ_2	$\Sigma_1 + \Sigma_2$
Sc180	0.0	5.3(3)	0.0	50.0(4)	5.3(3)	100(5)
Sc192	0.4(2)	10.1(2)	0.0	50.6(1)	10.1(2)	85(1)
Ti106	14.6(5)	28.4(2)	0.0	0.0	28.4(2)	95(1)
V66	31.7(4)	0.0(17)	0.0	0.0	0.0	93(6)
V91	66.3(5)[a]	4.9(2)	0.0	0.0	4.9(2)	102(7)
Cr65	55.2(3)	0.0	0.0	0.0	0.0	94(3)
Cr115	76.2(4)	0.0	0.0	0.0	0.0	99(3)
Cr93	60.4(6)	5.7(6)	0.0	0.0	5.7(6)	78(2)
Mn67	4.9(3)	11.0(2)	0.0	1.1(3)	11.0(2)	103(4)
Fe64	33.4(4)	8.7(3)	0.0	0.0	8.7(3)	101(5)
Co103	33.5(3)	15.5(2)	0.0	0.0	15.5(2)	85(4)
Ni135	1.0(2)	0.0	6.3(1)	0.0	12.6(2)	107(4)
Ni71	3.2(2)	3.3(2)	5.7(1)	0.0	14.7(4)	111(3)
Ni100	37.6(2)	3.8(4)	6.6(2)	0.0	17.0(8)	116(4)
Cu130	0.0	0.0	2.3(6)	0.0	4.6(12)	106(6)
Cu185	0.0	0.0	6.2(1)	4.2(2)	12.5(2)	110(3)
Zr37	1.7(2)0	8.1(1)	0.0	10.7(2)	8.1(1)	71(1)
Nb162	1.4(2)	8.3(1)	0.0	0.0	8.3(1)	96(5)
Hf174	0.0(1)	7.3(1)	0.0	6.5(2)	7.3(1)	84(2)
Hf169	0.5(2)	31.1(2)	0.0	9.8(2)	31.1(2)	97(3)
Ta170	2.5(1)	17.2(1)	0.0	0.0	17.2(1)	89(3)

[a] The A_2 site (18h) for sample V91 has an occupancy of $P = 0.8(2)\%$.

TABLE IVa

COORDINATES $\times 10^4$ OF THE B17 AND B18 ATOMS IN THE HEXAGONAL UNIT CELL OF β-BORON

	B17 (18h)		B18 (18h)	
	x[a]	z	x	z
Sc180	837(34)	4795(19)	1497(31)	5232(22)
V66	819(25)	4763(18)	1469(16)	5233(12)
V91	[852(9)]	4755(11)	1443(10)	5239(11)
Cr65	[853(24)]	4742(9)	1408(13)	5232(10)
Cr115	[837(26)]	4761(10)	1409(11)	5236(8)
Mn67	831(28)	4754(18)	1462(15)	5227(14)
Fe64	[863(23)]	4778(21)	1538(27)	5238(23)
Co103	900(32)	4746(26)	1481(18)	5195(16)
Ni135	874(14)	4754(12)	1521(9)	5223(7)
Ni71	[891(30)]	4746(12)	1542(11)	5224(9)
Ni100	[888(12)]	4751(7)	1518(7)	5218(6)
Cu130	[851(26)]	4747(23)	1663(18)	5293(13)
Cu185	[869(21)]	4738(9)	1518(10)	5223(8)
Nb162	[831(34)]	4748(18)	1530(29)	5247(25)
Ta170	[743(33)]	4762(32)	None	None
Pure 57	[852(32)]	4789(26)	1421(31)	5202(23)
Pure EP	833(14)	4760(11)	1440(7)	5239(5)
	$y = 2x$		$y = 2x$	

[a] The values in brackets are the equivalent x_E values from Table IVb.

IV. Results

IVA. Occupied Sites

The results for the partially occupied sites in the structure are given in Tables IIIa and IIIb where both partially occupied boron sites and dopant sites are listed. For the undoped β-boron sites we refer to the paper by Slack *et al.* (*23*) which lists 20 different fully and partially occupied boron positions in the unit cell, 4 more than given by previous authors (*21, 22*). The dopant atoms have been found to occupy A_1, A_2, D, Dd, and E sites (*3*). In the present notation Dd refers to a distorted or split D site, which has been seen previously for Ni (*6*) and Cu (*4, 7, 8*).

The *x*, *y*, *z* coordinates of the boron sites B17 and B18 and of the occupied dopant sites are given in Tables IVa, IVb, Va, and

TABLE IVb

COORDINATES $\times 10^4$ FOR B17d SITES AND THEIR CONVERSION TO EQUIVALENT HIGHER SYMMETRY B17 SITES

Sample	B17d (36i) x	y	z	Equivalent B17 (18h) x_E (Eq. 4)	Displacement (Å)
V91	493(19)	1659(21)	4755(11)	852(9)	0.37
Cr65	437(24)	1646(24)	4742(9)	853(24)	0.43
Cr115	398(26)	1605(26)	4761(10)	836(26)	0.45
Fe64	562(51)	1694(51)	4778(21)	863(23)	0.31
Ni71	620(29)	1757(32)	4746(12)	891(30)	0.28
Ni100	625(18)	1752(19)	4751(7)	888(12)	0.28
Cu130	667(60)	1728(63)	4747(23)	872(39)	0.22
Cu185	636(21)	1717(22)	4738(9)	868(10)	0.25
Nb162	505(47)	1624(50)	4748(18)	831(34)	0.33
Ta170	277(83)	1403(84)	4762(32)	743(33)	0.47
Pure 57	495(61)	1660(71)	4789(26)	852(32)	0.37

Vb. In the special case of undoped β-boron the coordinates for the vacant dopant sites are for those positions where the distances to the neighboring boron atoms are most nearly equal. The A_1 site has 12 boron neighbors: 6B1 + 3B5 + 3B7; the A_2 site also has 12: 2B1 + 2B2 + 2B3 + 2B5 + 1B6 + 2B7 + 1B8; the D site has 14: 2B1 + 4B2 + 4B3 + 1B12 + 2B13 + 1B15. In this listing for the D site we do not include the very close B13 site at 1.7 to 2.1 Å, which is probably empty when the nearest D site is filled. The Dd site has essentially the same collection of boron neighbors, since it is only displaced ~0.4 Å from the undistorted D site. The E site has 15 boron neighbors: 6B1 + 3B9 + 3B11 + 3B10. The boron sites have the same notation as that used by Hoard *et al.* (*22*), Callmer (*21*), and Slack *et al.* (*23*).

IVB. Percentage Site Occupancy

The boron sites B13, B16, B17, B18, B19,

TABLE Va

COORDINATES $\times 10^4$ FOR DOPANT SITES IN THE HEXAGONAL UNIT CELL OF β-BORON

Sample No.	A_1 (6c) z	A_2 (18h) x	z	E (6c) z	D (18h) x	z
Sc180	—			2341(1)	1304(5)	4930(4)
Sc192	1276(66)			2342(1)	1305(2)	4925(1)
Ti106	1345(3)				1349(1)	4903(1)
V66	1343.1(8)				—	—
V91	1341.6(4)	2223(16)	5640(15)		1344(3)	4920(3)
Cr65	1343.5(3)				—	—
Cr115	1343.9(3)				—	—
Cr93	1343.3(7)				1279(45)	5072(29)
Mn67	1341(2)			2324(21)	1342(2)	4879(2)
Fe64	1353(1)				1313(3)	4939(2)
Co103	1366(1)				1256(1)	4959(1)
Ni135	1362(16)				—	—
Ni71	1368(7)				1147(7)	4962(6)
Ni100	1364(1)				1167(5)	4953(4)
Cu185	—			2210(4)	—	—
Zr37	1347(9)			2341(2)	1321(2)	4917(1)
Nb162	1350(10)			—	1352(1)	4912(1)
Hf174	—			2339(2)	1334(1)	4905(1)
Hf169	1349(23)			2336(1)	1327(1)	4905(1)
Ta170	1365(3)			—	1346(1)	4914(1)
Pure EP	1349	2243	5627	2370	1313	4932
	$x = y = 0$	$y = 2x$		$x = y = 0$	$y = 2x$	

TABLE Vb

COORDINATES $\times 10^4$ FOR Dd DOPANT SITES AND THEIR CONVERSION TO EQUIVALENT HIGHER SYMMETRY D SITES

Sample No.	Dd (36i) x	y	z	Equivalent D (18h) x_E	Displacement (Å)
Ni135	1472(3)	2215(3)	5003(1)	1127(2)	0.40
Ni71	1539(6)	2189(5)	5012(2)	1124(3)	0.49
Ni100	1521(5)	2198(3)	5008(1)	1126(2)	0.47
Cu130	819(10)	2320(11)	5012(4)	1177(7)	0.38
Cu185	1504(3)	2278(3)	5013(1)	1159(2)	0.40
				$y_E = 2x_E$	
				$z_E = z$	

and B20 are only partially occupied in undoped β-boron (*23*). The presence of foreign atoms in the structure changes the percentage occupancy of these sites, usually decreasing them, but occasionally increasing them. The results are discussed as follows:

Sites B13, B16, B17, B18, B19, and B20. As discussed by Slack *et al.* (*23*) the occupancies of these sites in pure β-boron are all related. This continues to be true in the doped samples.

Site B13. In undoped β-boron the B13 site is about 75% occupied (*23*). The vacant B13 sites are associated with the presence of B17 plus B18 pairs or with B19 atoms (see Slack *et al.* (*23*)). Table VIa gives the values for the distance from B17 to the unoccupied B13 site in a number of samples.

TABLE VIa

DISTANCE FROM THE CENTER OF THE UNDISTORTED B17 SITE TO THE TWO NEAREST UNOCCUPIED B13 SITES

Sample No.	Distance (Å)
Sc180	1.617(32)
V66	1.558(66)
Mn67	1.574(28)
Co103	1.658(70)
Ni135	1.637(18)
Pure EP	1.572(22)

These distances are generally too short for boron–boron bonds. In doped β-boron the occupancy of B13 varies from 63 to 77% and is low when the D site occupancy is high. The distance from the D site to the nearest B13 site is 1.7 to 2.1 Å, which is too short for a transition-metal–boron bond length. Thus we believe that each undistorted D site must have at least one neighboring B13 vacancy. Since there are probably never more than two vacant B13 sites out of the six in one rhombohedral unit cell, the minimum B13 occupancy is probably $\frac{4}{6} = 66.7\%$. This supposition agrees well with the observations in Table III. If this supposition is correct, then the maximum site occupation percentage for undistorted D sites is $\frac{1}{3} = 33.3\%$. The maximum found in Table III is 31.1% for Hf. If the B16 occupancy is still 27%, as in undoped β-boron, then there will be 313.9 boron atoms and six D-site dopant atoms in a hexagonal unit cell. We assume B17, B18, B19, and B20 are vacant. This gives a maximum dopant concentration of 1.88 atom% for elements which occupy only the D sites.

A corollary of this model is that the D site atoms compete with the B17–B18 pairs for the vacant B13 sites. Thus dopant atoms in D sites are not truly interstitials since they displace boron atoms, but they do not displace boron from the icosahedra of the main framework. The following sum of percentage occupancies for distorted and undistorted D sites has an upper limit:

$$2P(\mathrm{Dd}) + P(\mathrm{D}) + P(\mathrm{B18}) \leq 33.3\%. \quad (2)$$

The maximum value of this sum in Table III is 33.2% for sample Ni100.

Site B16. The B16 site is the interstitial site labeled G by Andersson and Lundström (*3*). It is only partially occupied by boron atoms in undoped β-boron. The distances to the eight surrounding boron atoms are too small for this site to accept transition-metal atoms. This site is in the center of three of the four hexagonal faces (of the truncated tetrahedron) that form the

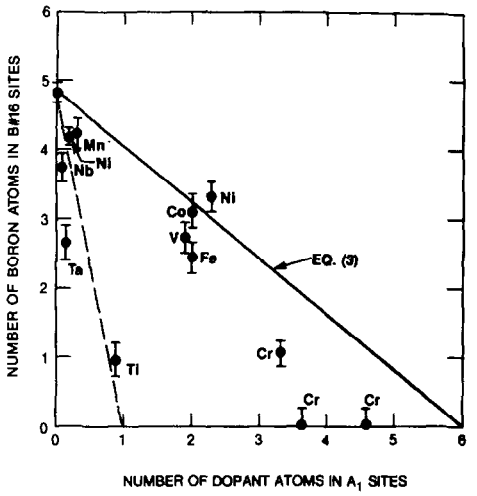

FIG. 1. Displacement of B16 atoms by dopants in the A_1 site. Values are the number of atoms in the hexagonal unit cell.

walls of the A_1 site. As such, it is only 1.135 Å away from the center of the A_1 site. Thus we do not expect that neighboring B16 and A_1 sites will be simultaneously occupied. The B16 site occupancy in undoped β-boron is 27% according to Slack *et al.* (*23*) or 24.8% according to Callmer (*21*). Thus there are 4.86 atoms of B16 in the hexagonal unit cell. If a dopant atom on the A_1 site prevents the three neighboring B16 sites from being occupied, it effectively displaces 0.81 boron atoms, that is, $3 \times 27\%$. The displacement balance equation can be written as:

$$n(\text{B16}) = 4.86 - 0.81[n(\text{A}_1)], \quad (3)$$

where n is the number of atoms of a particular kind in the hexagonal unit cell. We have plotted n(B16) versus $n(A_1)$ in Fig. 1 for those samples where only A_1 or D (also Dd) sites are occupied. The experimental data are from Table III. The agreement with Eq. (3) is reasonably good for V, Cr, Mn, Fe, Co, Ni. For Ti, Nb, and Ta the B16 displacement occurs much more rapidly, but we do not have a simple model to account for this effect. See the dashed line in Fig. 1. We conclude that A_1 dopant-site atoms displace boron B16 atoms.

Site B17. As in undoped β-boron we believe that B17 and B18 atoms generally occur in pairs. This pair bridges the gap between the two B_{28} units at the center of the rhombohedral unit cell. The concept of B_{12} and B_{28} units or clusters is discussed further in Sections V and VI. The arrangement is shown in Fig. 3 of the previous paper (*23*). Each B17 is bonded to 1B18 as well as to 1B12 + 1B13 + 1B15. Note that all of these boron–boron bonds to B17 lie in the same $(1\bar{2}10)$ plane. Thus it is relatively easy for the B17 atom to be displaced in a direction perpendicular to this plane to produce a distorted or B17d site (a 36i position) because only bond-bending distortions but no bond-stretching ones are required. In undoped β-boron we believe that an undistorted B17 position (an 18h) is occupied only when both B13E and B13D are vacant because both of these sites are only 1.572 Å away (Fig. 3 of (*23*); Table VIa). However, if B13D is occupied and B13E is vacant, then the B17 atom would be displaced by 0.30 Å to a B17d position where the B13D to B17d distance is 1.77 Å, a reasonable distance for a boron–boron bond. Table VIb gives the boron distances from the center of a B17d site to neighboring boron sites. Note that there is only one unacceptably short distance, which is to B13E. Thus this single B13 site is probably vacant. We believe that B17d positions arise when only a single B13 vacancy appears and a double B13 vacancy is unavailable. A comparison of samples Ni135 and Ni71 shows that B17 positions are occupied in the slowly cooled sample Ni135, while B17d positions occur in the rapidly cooled sample Ni71. So B17 positions may be nearer to the equilibrium configuration than distorted B17d positions. This has also been found in undoped β-boron (*23*).

In Tables IIIa and IVb are listed the samples for which B17d boron atoms were

TABLE VIb

NEAREST-NEIGHBOR DISTANCES IN Å FROM THE CENTER OF THE DISTORTED B17d SITE TO OTHER PROBABLY OCCUPIED BORON SITES[a]

Sample No.	B12	B13D	B13A	B13E[b]	B15	B18
V91	1.885(29)	1.814(29)	1.987(29)	1.383(26)	1.721(24)	1.682(33)
Cr65	1.857(22)	1.837(21)	2.010(22)	1.331(15)	1.735(10)	1.666(34)
Cr115	1.917(25)	1.846(34)	1.972(26)	1.321(22)	1.690(29)	1.677(30)
Fe64	1.912(52)	1.814(54)	1.910(53)	1.450(59)	1.720(67)	1.736(71)
Ni71	1.838(31)	1.814(26)	2.054(32)	1.495(37)	1.797(34)	1.721(36)
Ni100	1.847(20)	1.815(25)	2.052(21)	1.508(17)	1.789(21)	1.674(23)
Cu130	1.826(56)	1.741(54)	1.978(55)	1.484(19)	1.761(53)	2.012(66)
Cu185	1.823(24)	1.748(29)	2.029(25)	1.461(70)	1.761(24)	1.721(29)
Nb162	1.852(45)	1.762(41)	1.984(43)	1.359(57)	1.685(42)	1.838(76)
Pure 57	1.939(62)	1.840(85)	1.873(65)	1.409(53)	1.690(75)	1.977(77)

[a] In all cases there is only one boron atom at the given distance.
[b] This boron site is probably vacant when B17d is occupied.

found. Because the distortion from a true B17 site is so small, we have established an equivalent undistorted B17 position for each B17d example. This equivalent position was established by maintaining z constant and by maintaining a constant B15 to B17 distance. In Table IVb we list the displacement distance in the hexagonal a–b plane required to move from B17d to B17. The observed values are close to 0.35 Å. The equivalent coordinates x_E, y_E, and z_E are given by:

$$3(x_E)^2 = x^2 + y^2 - xy, \qquad y_E = 2x_E, \quad z_E = z \tag{4}$$

The maximum B17 occupancy depends on the availability of B13 vacancies. The minimum B13 occupancy is ~66.7% corresponding to two vacancies per rhombohedral cell. One undistorted B17 site requires two adjacent B13 vacancies. Thus a maximum of one out of six possible B17 sites can be occupied in a rhombohedral cell, so the maximum occupancy is 16.7%. For each B17d site only one B13 vacancy is needed, so that the maximum possible occupancy is two occupied B17d sites per rhombohedral cell out of a total of 12. This again gives 16.7% maximum occupancy of B17d sites. Note that the upper limit on the occupancy of B18 would be 33% if B17d occurs in pairs with B18.

In those cases where boron atoms have been detected we note that for many cases:

$$P(17) + 2P(17d) \simeq P(18). \tag{5}$$

This relationship agrees with the concept that the boron atoms usually occur in pairs. This may not be true for Cu130 or Nb162.

Let us define an occupancy sum Σ_1 by:

$$\Sigma_1 = P(B13) + P(B17) + 2P(B17d) + P(B18) + P(B19). \tag{6}$$

In pure β-boron, $\Sigma_1 = 96 \pm 3\%$ from Table III. Thus sometimes it is close to its maximum value of 100%.

In Table III we see that no boron atoms were detected in site B19 for the doped samples and that Σ_1 is always $\leq 100\%$. In many cases we believe that boron may be present in these sites, but at levels indistinguishable from the noise. From Table Ia this varies from 2 to 8% of a boron atom depending on the sample. So very few conclusions should be drawn from very low or apparent absence of occupancy of B17,

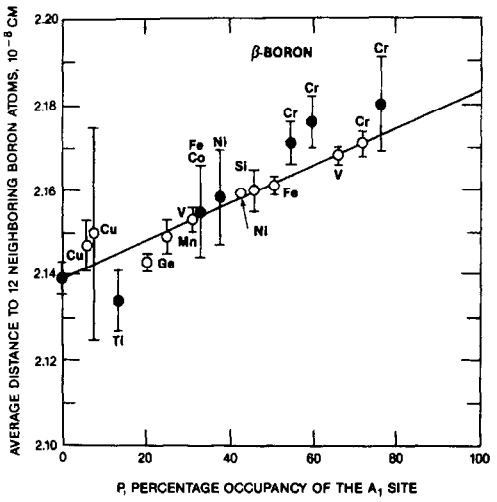

FIG. 2. Average distance from the center of the A_1 site to the 12 nearest-neighbor boron atoms. The filled circles are the present data; the open ones are from Garbauskas *et al.* (*2*).

B17d, B18, B19, or B20 in these doped samples. When their presence is reported, it is most probably true.

Site B18. In undoped β-boron the boron atoms in B18 sites are bonded to four other boron atoms: B3A + B3B + B13A + B17 (see Fig. 3 of (*23*)). Note that, in contrast to B17, not all of these bonds are in the $(1\bar{2}10)$ plane. Thus the B18 position is well fixed, and no distorted (lower symmetry) B18 sites were observed; they are all 18h sites. A distorted B18 site would require changes in boron–boron bond lengths, while a distorted B17 site only requires changes in bond angles. Thus B18 sites are more stable against distortion than B17 sites. The x and z coordinates for the observed B18 sites are given in Table IVa. They are close to but not identical with those in undoped boron. The maximum shift in the B18 position from undoped to doped boron occurs for Cu130 where it amounts to 0.45 Å. For Cr65 the shift is only 0.13 Å. But in all cases the B18 atom remains in an 18h site and lies in the $(1\bar{2}10)$ plane.

The upper limit on the occupancy of B18 is linked to that of B17. For B17–B18 pairs this limit is 16.7%, or three pairs per hexagonal unit cell, as discussed under the B17 site section. For B17d–B18 pairs it may be as high as 33.3%, or six pairs per hexagonal unit cell. None of the entries in Table III exceed these limits.

Sites B19 and B20. There is very little evidence of B19 or B20 site occupancy in the doped β-boron samples. As discussed by Slack *et al.* (*23*) the occupancy of B19 is probably associated with only a single vacancy in the B13 sextet, or a B13 occupancy of 83.3%. The doped samples generally produce a decrease in the B13 occupancy toward 66.7%. Thus B19 occupancy is expected to decrease as the B13 occupancy decreases below 75%. This is not contradicted by the present observations. Since B19 and B20 sites are close to B16 sites (*23*), their occupancy may also decrease as P(B16) decreases.

In sample Cu130, the position for B18 given in Table IVa is actually intermediate between B18 and B19 in undoped boron. Thus at 0.26 atom% Cu there is some evidence of a low B19 occupancy. However, in this sample the B18 and B19 positions are not separately resolvable.

Site A_1. In undoped β-boron the average distance from the center of the A_1 site to the 12 neighboring boron atoms at the corners of a truncated tetrahedron is 2.139 Å (see Table VIIa). This average distance generally increases as the A_1 site occupancy increases, as shown in Fig. 2. All of the first-row transition metals from Ti to Cu as well as Ga and Ge will enter the A_1 site. The open circles are from Garbauskas *et al.* (*2*); the closed circles are data points from Table VIIa. The general trend is the same for all of the metals and shows that the maximum expansion is 2.183 Å. The local lattice expansion produced by these various elemental dopants appears to depend only on the boron structure and does not correlate with the elemental radii of the dopant atoms. In Table VIII are listed the metal-to-

TABLE VIIa

DISTANCES IN Å FROM THE CENTER OF THE A_1 SITE TO NEIGHBORING BORON SITES

Sample No.	6B1	3B5	3B7	Average Distance	P
Sc192	2.201(52)	2.027(85)	2.112(20)	2.135(52)	0.4
Ti106	2.133(6)	2.135(8)	2.134(6)	2.134(7)	14.6
V66	2.166(11)	2.134(11)	2.147(11)	2.153(11)	31.7
V91	2.185(1)	2.143(2)	2.160(2)	2.168(2)	66.3
Cr65	2.188(5)	2.148(5)	2.159(5)	2.171(5)	55.2
Cr115	2.199(11)	2.153(11)	2.169(11)	2.180(11)	76.2
Cr93	2.196(6)	2.149(6)	2.164(6)	2.176(6)	60.4
Mn67	2.143(7)	2.153(11)	2.146(11)	2.146(10)	4.9
Fe64	2.154(11)	2.156(11)	2.157(11)	2.155(11)	33.4
Co103	2.140(11)	2.184(11)	2.158(11)	2.156(11)	33.5
Ni135	2.130(20)	2.171(35)	2.144(14)	2.144(22)	1.0
Ni71	2.112(13)	2.178(18)	2.153(12)	2.144(14)	3.2
Ni100	2.145(11)	2.181(11)	2.158(11)	2.157(11)	37.6
Zr37	2.145(15)	2.141(22)	2.139(12)	2.143(16)	1.7
Nb162	2.132(12)	2.138(22)	2.135(8)	2.134(14)	1.4
Hf169	2.140(5)	2.117(6)	2.131(7)	2.132(6)	0.5
Ta170	2.112(6)	2.176(9)	2.145(6)	2.136(7)	2.5
Pure EP	2.142(2)	2.136(3)	2.137(2)	2.139(2)	0.0

TABLE VIIb

DISTANCES IN Å FROM THE CENTER OF THE A_2 SITE TO NEIGHBORING BORON SITES

Atoms	Pure EP	V91
2B1	2.014(2)	2.066(34)
2B2	2.100(2)	2.099(19)
2B3	2.053(2)	2.023(29)
2B5	2.118(2)	2.144(31)
1B6	2.203(2)	2.189(38)
2B7	2.085(2)	2.119(19)
1B8	2.152(2)	2.113(37)
Avg.	2.091(2)	2.100(28)

boron distances for various pairs of metal atoms and boron. These distances have been taken from MB, MB_2, or MB_4 compounds or, when these are not available, from the sum of the elemental radii (25). From this table, we see that Hf is about the largest atom found to enter an A_1 site. The maximum Hf percentage occupation in an A_1 site is only 0.5% from Table III.

The correlation of the A_1 occupancy with the B16 occupancy has been discussed under B16. If only the A_1 sites are occupied to their maximum extent of six sites per hexagonal unit cell and if they alter only the B16, B19, and B20 occupancies, then the unit cell will contain 314.6 boron + 6 dopant atoms for a maximum dopant concen-

TABLE VIIc

DISTANCES IN Å FROM THE CENTER OF THE D SITE TO OTHER NEIGHBORING, PROBABLY OCCUPIED BORON SITES

Sample No.	2B1	2B2	2B2	2B3	2B3	1B12	2B13 (E or D)	1B15	Average	P
Sc180	2.383(15)	2.392(13)	2.406(13)	2.292(14)	2.454(14)	2.373(15)	2.417(15)	2.473(16)	2.395(14)	5.3
Sc192	2.393(12)	2.405(12)	2.411(12)	2.315(12)	2.459(13)	2.369(12)	2.422(13)	2.482(13)	2.404(12)	10.1
Ti106	2.326(6)	2.359(6)	2.396(6)	2.359(6)	2.426(6)	2.355(6)	2.473(8)	2.563(5)	2.400(6)	28.4
V91	2.321(13)	2.379(12)	2.380(12)	2.321(13)	2.459(13)	2.390(14)	2.483(14)	2.561(14)	2.403(13)	4.9
Cr93	2.476(79)	2.289(45)	2.553(43)	1.991(61)	2.708(56)	2.690(71)	2.567(76)	2.442(86)	2.450(63)	5.7
Mn67	2.332(6)	2.354(5)	2.418(6)	2.399(6)	2.401(6)	2.308(16)	2.445(6)	2.564(6)	2.398(12)	11.0
Fe64	2.374(13)	2.382(13)	2.412(13)	2.272(13)	2.471(13)	2.398(14)	2.444(13)	2.496(14)	2.400(13)	8.7
Co103	2.489(13)	2.411(12)	2.474(12)	2.235(11)	2.497(13)	2.418(13)	2.402(13)	2.385(12)	2.416(13)	15.5
Ni71	2.676(19)	2.514(16)	2.570(15)	2.247(17)	2.484(16)	2.376(18)	2.261(17)	2.179(17)	2.433(17)	14.7[a]
Ni100	2.642(16)	2.506(14)	2.550(14)	2.262(14)	2.475(14)	2.360(15)	2.285(14)	2.220(14)	2.430(14)	17.0[a]
Zr37	2.363(12)	2.388(12)	2.399(12)	2.337(12)	2.451(13)	2.373(13)	2.440(13)	2.511(13)	2.403(12)	8.1
Nb162	2.315(6)	2.362(5)	2.377(5)	2.332(5)	2.443(6)	2.366(6)	2.479(6)	2.569(6)	2.397(6)	8.3
Hf174	2.348(6)	2.372(5)	2.401(6)	2.360(6)	2.432(6)	2.346(7)	2.442(8)	2.540(6)	2.400(6)	7.3
Hf169	2.378(6)	2.401(6)	2.435(6)	2.391(6)	2.456(6)	2.383(6)	2.462(7)	2.531(5)	2.426(6)	31.1
Ta170	2.333(6)	2.366(5)	2.385(5)	2.337(5)	2.445(5)	2.373(6)	2.474(7)	2.558(5)	2.401(6)	17.2
Pure EP	2.372(2)	2.379(2)	2.398(2)	2.281(2)	2.457(2)	2.376(2)	2.430(2)	2.491(2)	2.393(2)	0.0

[a] These are Σ_2 values.

TABLE VIId

DISTANCE IN Å FROM CENTER OF D SITE TO NEARBY PROBABLY UNOCCUPIED SITES

Sample No.	B13A (boron)	Nearest D (metal)
Sc180	1.997(14)	2.490(23)
Sc192	2.018(11)	2.501(13)
Ti106	2.152(7)	2.594(6)
V91	2.103(13)	2.582(13)
Cr93	1.747(80)	2.460(24)
Mn67	2.164(7)	2.612(13)
Fe64	2.002(12)	2.509(13)
Co103	1.933(11)	2.391(12)
Ni71	1.807(17)	2.185(17)
Ni100	1.860(13)	2.229(11)
Zr37	2.063(12)	2.535(13)
Nb162	2.112(7)	2.595(7)
Hf174	2.098(8)	2.570(7)
Hf169	2.146(9)	2.563(5)
Ta170	2.114(7)	2.584(5)
Pure EP	2.003(2)	2.507(3)

tration of 1.87 atom%. For higher metal–atom concentrations other sites must be occupied. The distance from the A_1 site to the E site is ≤2.43 Å in the samples studied. This distance is too small for metal atoms to occupy adjacent A_1 and E sites. Thus completely filled A_1 sites mean completely vacant E sites. There is no such competition between A_1 and D sites.

TABLE VIIe

DISTANCES IN Å FROM THE CENTER OF THE Dd SITE TO NEIGHBORING, PROBABLY OCCUPIED BORON SITES (RANGE 2.0 TO 2.7 Å)

Neighbor	Ni 135	Ni 71	Ni 100	Cu 130	Cu 185
B1	2.642(14)	2.654(14)	2.647(14)	2.553(18)	2.581(13)
B2	2.236(12)	2.189(12)	2.206(12)	2.180(18)	2.184(11)
B2	2.326(12)	2.288(13)	2.302(12)	2.299(18)	2.299(12)
B3	2.028(11)	1.991(11)	2.005(11)	1.998(15)	2.005(11)
B3	2.311(12)	2.282(13)	2.292(12)	2.328(16)	2.341(12)
B3	2.374(12)	2.413(14)	2.405(13)	2.348(16)	2.354(12)
B12	2.490(13)	2.524(14)	2.510(13)	2.523(16)	2.536(13)
B13A	2.124(12)	2.106(11)	2.122(11)	2.190(15)	2.172(12)
B13E or D	2.449(13)	2.500(14)	2.494(13)	2.497(18)	2.493(13)
B15	2.138(11)	2.133(12)	2.139(11)	2.234(16)	2.196(11)
B17	2.306(18)				
B17d		2.130(30)	2.118(20)	2.145(81)	2.117(23)
B18	2.265(16)	2.208(35)	2.202(25)	2.548(23)	2.284(17)
Avg.	2.312(13)	2.308(13)	2.287(14)	2.315(17)	2.316(12)
% Occupancy	6.3	5.7	6.6	2.3	6.2

Note. The B17 or B17d sites listed in the table may actually be occupied. The average distance is calculated omitting B17, B17d, and B18 distances.

TABLE VIIf

DISTANCES IN Å FROM THE CENTER OF THE E SITE TO NEIGHBORING BORON SITES

Sample No.	6B1	3B9	3B10	3B11	Avg.	*P*
Sc180	2.365(12)	2.450(12)	2.511(13)	2.484(13)	2.435(12)	50.0
Sc192	2.373(12)	2.453(12)	2.518(13)	2.488(13)	2.441(12)	50.6
Mn67	2.322(27)	2.440(6)	2.550(31)	2.493(42)	2.425(27)	1.1
Cu185	2.177(12)	2.455(12)	2.728(16)	2.739(17)	2.455(14)	4.2
Zr37	2.352(12)	2.441(13)	2.527(13)	2.466(13)	2.428(13)	10.7
Hf174	2.336(6)	2.433(7)	2.524(7)	2.453(7)	2.416(7)	6.5
Hf169	2.341(6)	2.445(6)	2.530(7)	2.477(7)	2.427(6)	9.8
Pure EP	2.379(2)	2.437(2)	2.468(3)	2.386(3)	2.408(2)	0.0

TABLE VIII

METAL–BORON DISTANCES AND SITE OCCUPATIONS FOR DIFFERENT DOPANT CONCENTRATIONS

Dopant	*M*–B distance (Å)	Site occupation[a] A_1	A_2	D	E	Other
Si	2.09	X	X			X
Ge	2.13	X	X	X		X
Ni	2.15	H		L		
Co	2.15	X		X		
Fe	2.16	L		H		
Cu	2.17	H		L	M	
Cr	2.30	L		H		
Mn	2.31	L		L	H	
V	2.31	L	H	H		
Al	2.38	L				
Ti	2.38	X		X		
Ta	2.41	H		L		
Nb	2.43	H		L		
Ga	2.44	X		X		
Mg	2.49	H		L	L	
Sc	2.50	H		M	L	
Hf	2.51	H		L	M	
Zr	2.54	H		L	M	
Lu, etc.	≥2.64	(not soluble)				

[a] X, Occupied; L, occupied at low dopant concentration; M, occupied at medium dopant concentration; H, occupied at high dopant concentration.

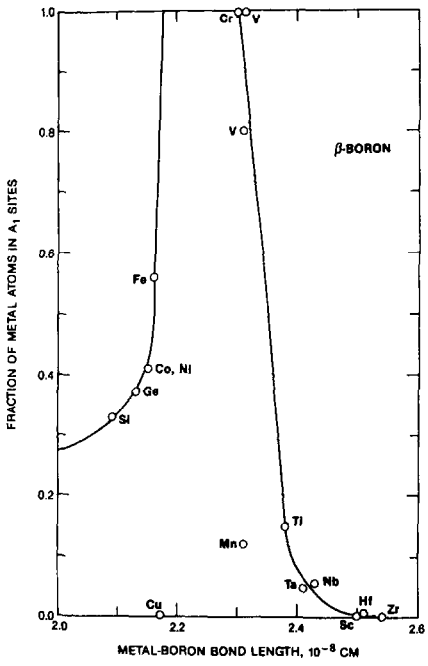

FIG. 3. Fraction of dopant M atoms in the A_1 site versus M–B distances from Table VIII. For most metals the data are for a total concentration of ~1 atom% and for slowly cooled samples when known.

The elements of the first transition metal series, Sc to Cu, have different site occupancy preferences. If we consider a doping level of 1 to 2 atom%, we can calculate the fraction of the dopant atoms that enter the A_1 site. Even though this fraction depends somewhat on the total concentration and the cooling rate, some trends are discernible. From our data we have chosen the slowly-cooled samples. Figure 3 gives the results derived from Table III and Refs. (*1, 9, 11, 12*). For Si the data (*10*) are for 2.7 atom%.

It can be seen in Fig. 3 that the intermediate size atoms such as Cr and V fit well into the A_1 site. Other atoms are either too large or too small. For Cu and Mn size does not determine the behavior; maybe electron-transfer effects are important here.

Site A_2. The A_2 site is partially occupied only for sample V91 which contains 1.57 atom% vanadium. The transition elements in Table VIII with apparent radii smaller than that of V do not enter this site. The only elements previously found in the A_2 sites are Si (*11*) and Ge (*12*). The average dopant-to-boron distances found were:

Si: 2.096(10) Å
Ge: 2.084(10) Å

These are comparable to the values for undoped and V-doped samples in Table VIIb. In all cases the percentage occupancy of the A_2 site was ≤4.8%. This site is somewhat smaller than the A_1 site. If we give boron a radius of 0.88 Å, then the radius of the A_2 hole is 90% of the radius of the A_1 hole in undoped β-boron. It is thus the smallest site for which we have measured a partial occupancy.

Site D. The D site is shown in Fig. 4 in relation to B13, B15, and other nearby atoms. To a first approximation a dopant atom in the D position excludes boron atoms from the B17, B18, and B19 sites (see Fig. 3 of Ref. (*23*)). In undoped β-boron the distance between the D site and its boron neighbors is 2.393 Å (see Table VIIc). The

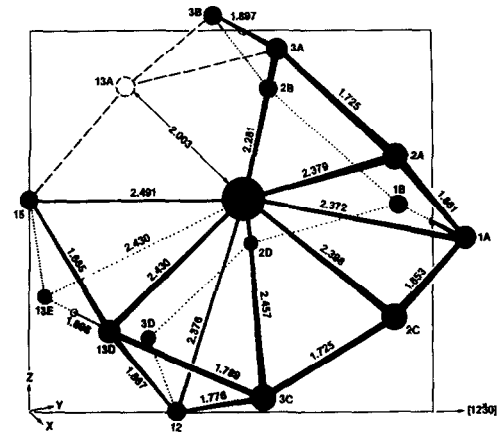

FIG. 4. The local environment of a dopant in the undistorted D site (large atom in center) in β-boron. The boron position 13A is vacant because 2.003 Å is too short for a metal–boron bond. The bond distances are characteristic of a very lightly doped crystal. Compare with Fig. 3 of (*23*). The D-site dopant displaces boron atoms B17 and B18.

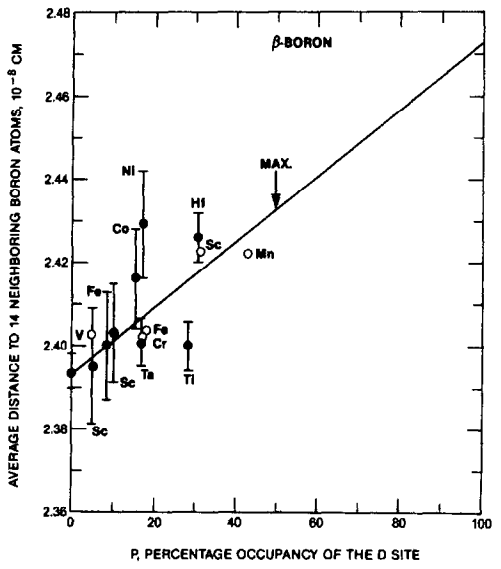

FIG. 5. Average distance from the center of the D site to the 14 nearest-neighbor boron atoms. The filled circles are the present data; the open ones are from Garbauskas *et al.* (*2*).

distance to site B13A is 2.005 Å (see Table VIId). This distance to B13A is too short for both sites to be simultaneously occupied by boron and a transition metal. Thus a filled D site requires one neighboring B13A vacancy, and the maximum percentage occupancy of D sites is expected to be 33.3%. For Sc, Callmer (*1*) found 31.4% at the maximum Sc concentration. For Mn this rule appears to be violated; the maximum occupancy found (*4*) was 43.1%.

In Cu-doped and Ni-doped β-boron we find distorted D sites, which we label Dd sites. As shown in Table Vb these are displaced from the D sites by 0.4 to 0.5 Å. The equivalent undistorted x_E and y_E values are calculated from Eq. (4). These Dd sites occupy a general position, 36i, in the structure and are related to the higher symmetry 18h D sites. We believe that these Dd sites are produced from an undistorted D site by the presence of a nearby boron atom in the usually vacant B13A position. Define the sum:

$$\Sigma_2 = P(\mathrm{D}) + 2P(\mathrm{Dd}) \qquad (7)$$

If the interference of a dopant atom with a boron atom in B13A is avoided by the distortion, then the maximum value of Σ_2 will be 50%. This limit is imposed by metal–metal atom overlap (*4*). In fact in CuB_{23} Higashi *et al.* (*7*) found a Σ_2 of 46%. With a Σ_2 value of 50%, the maximum dopant content for those atoms which occupy only D sites is just 2.79 atom%.

The replacement of B17–B18 pairs by D-site dopants sets an upper limit on the sum $\Sigma_1 + \Sigma_2$. At the maximum value of Σ_2 of 50% we expect that Σ_1 will have its minimum value of just P(B13) of 66.7%. Thus we believe that the upper limit on $\Sigma_1 + \Sigma_2 =$ 116.7%. From Table III we see that sample Ni100 comes close to this limit at $\Sigma_1 + \Sigma_2 =$ 111%; the other samples are all less than this limit. Another consequence of the B17–B18 replacement is that Σ_3, which we define by

$$\Sigma_3 = \Sigma_1 + \Sigma_2 - P(\mathrm{B13}) - P(\mathrm{B19}),$$

has a nearly constant value. Note that Σ_3 is equal to:

$$P(\mathrm{B17}) + 2P(\mathrm{B17d}) + P(\mathrm{B18}) + P(\mathrm{D}) + 2P(\mathrm{Dd})$$

and this sum has a more or less constant value of:

$$\Sigma_3 = 26(6)\% \text{ for most samples}$$

$$\Sigma_3 = 37(5)\% \text{ for Ni-, Cu-doped samples.} \qquad (8)$$

If we assume that the nearest-neighboring B13 site is vacant, then the average distance from an undistorted D site to the 14 neighboring boron atoms is 2.393 Å in undoped β-boron. From Table VIII this site is large enough to accommodate all of the first transition-metal series, but is a little small for Sc, Hf, and Zr. However, from Fig. 5 we find, again, that the site expansion depends primarily on the fractional occupancy, but not on the size of the elemental atom. The solid circles are the present data

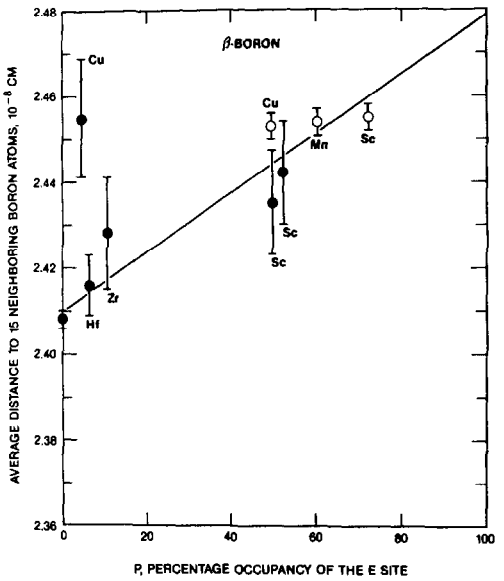

FIG. 6. Average distance from the center of the E site to the 15 nearest-neighbor boron atoms. The filled circles are the present data; the open ones are from the literature (*1*, *4*).

from Table VIIc, the open ones are from the literature (*2*). For Ni in Fig. 5, we used Σ_2, the total occupancy of the D and Dd sites.

For the D sites at 100% occupancy (see Fig. 5), the average boron distance is 2.47 Å. This means that the D sites can contain atoms or ions up to a radius of 1.59 Å. This is 22% larger than the A_1 site where the maximum hole radius is 1.30 Å at full occupancy. At zero occupancy it is 20% larger than A_1.

The Dd sites have an average boron–metal distance about 0.1 Å less than the undistorted D sites (see Table VIIe). The Dd sites only occur for Ni and Cu atoms, which are at the small end of the size range in Table VIII. The larger atoms such as Zr and Hf do not occupy Dd sites, thus they require a B13A vacancy when in a D site.

Site E. The data on E site occupancy are much less extensive than that for A_1 and D sites. The 15 neighboring boron distances are given in Table VIIf. The average distance is plotted in Fig. 6. From the literature we have data for Cu and Mn (*4*) and Sc (*1*). The undoped β-boron has the E site x, y, z parameters listed in Table Va. These were derived to give the most nearly equal distances to the 15 neighboring atoms. The present data for Hf, Zr, and Sc fit the best straight line through all of the points fairly well. They are typical E site occupants.

The E site is larger than the A_1 or D site, and appears to have a maximum metal–boron distance of 2.48 Å. It is about 21% larger than the A_1 site in undoped β-boron. From Table VIII, we see that Zr is the largest ion that is known to incorporate in β-boron. The larger ions such as Lu, Y, and Ca appear not to be soluble in β-boron at concentrations of ~1 atom%. At this concentration Lu and Y alter the β-boron structure to that of $B_{68}Y$ (*26*).

There appears to be some influence of E-site dopants on the occupancy of B16. In general they decrease the B16 occupancy. The E to B16 distance is 2.99 Å, so that the argument used for Eq. (3) is no longer valid. The coupling may be via donated electrons. Figure 7 shows the number of B16 atoms in a hexagonal unit cell versus the number of E-site dopants. The straight line fits the Sc points. The Hf and Zr, which may donate one more electron per atom than Sc, replace B16 atoms more rapidly, while Cu is much less effective.

IVC. Characteristics of Various Transition Metals

Here we review the present results for each element and compare them with other results from the literature. The general effect of most of the transition elements is to donate electrons to the electron-deficient β-boron structure. One way this donation shows up is in the increased electron concentrations near the center of the intercluster bonds. This local electron concentration has been seen in undoped β-boron (*23*); in

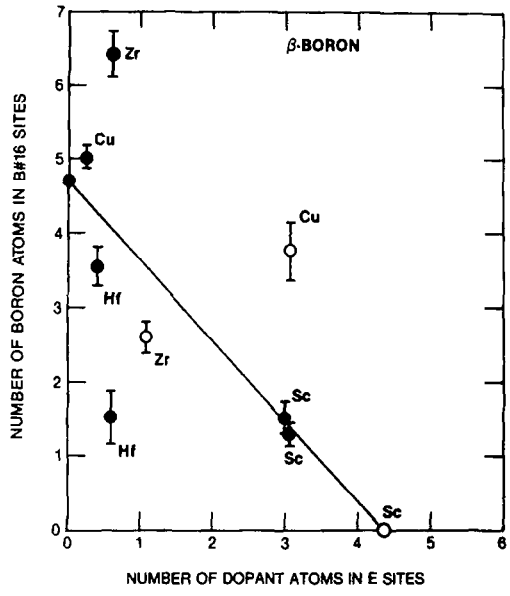

FIG. 7. Displacement of B16 atoms by dopants in the E site. Values are the number of atoms in the hexagonal unit cell. The filled circles are the present data; the open circles are from the literature: Sc (*1*), Cu (*4*), Zr (*9*).

the doped samples this concentration usually increases. In the Cu-doped samples (Cu185), however, it appears to decrease; which agrees with the electrical observation that Cu at low concentrations is not a donor but is actually an electron acceptor in β-boron. The measured electron densities in electrons/10^{-24} cm^3 at the centers of the intercluster bonds for the most heavily doped samples are given in Table IX. Of the seven bonds listed only the B1–B1 and B13–B15 bonds fail to show this effect. For scaling purposes, the peak electron density at the center of a boron atom is about 20 e/10^{-24} cm^3. The electron densities in Table IX are close to our detectability limit and have uncertainties of ±30%.

We believe that this increased electron density has been misinterpreted as actual metal atoms substituting for B4–B4 pairs in Sc-doped (*1*) and Zr-doped (*9*) β-boron. Neutron scattering or precision density measurements could presumably be used to

TABLE IX

ELECTRON DENSITY NEAR THE CENTER OF INTERCLUSTER BONDS (ELECTRONS/10^{-24} cm^3)

	Bond						
Sample No.	B1–B1	B2–B3	B4–B4	B5–B7	B6–B8	B9–B10	B13–B15
Sc180	—	0.33	0.39	0.39	0.44	0.37	—
Sc192	0.36	0.44	0.63	—	0.61	0.39	—
Ti106	0.39	0.29	0.32	—	0.38	0.35	—
V91	—	0.42	0.40	0.32	—	0.46	—
Cr115	—	0.30	0.46	0.24	0.32	0.37	0.28
Cr93	—	0.75	0.93	0.68	0.63	0.70	—
Mn67	0.35	0.36	—	0.39	0.48	0.28	—
Fe64	—	0.47	0.86	—	0.62	0.50	—
Co103	0.38	—	0.68	—	0.76	0.51	—
Ni100	0.29	0.36	0.56	0.39	0.36	0.39	—
Cu185	0.29	0.31	0.31	0.28	0.39	0.30	0.24
Zr37	0.35	0.38	0.35	0.35	—	0.33	—
Nb162	—	0.32	0.33	0.47	0.43	0.45	0.27
Hf169	—	—	—	0.57	—	0.74	—
Ta170	0.46	—	0.45	—	0.35	0.53	0.28
Pure 57	0.28	0.38	0.37	0.32	0.38	0.36	0.27
Pure EP	0.36	0.46	0.39	0.42	0.49	0.37	0.29

TABLE X

SOLUBILITY LIMITS FOR SOME TRANSITION METAL ELEMENTS IN β-BORON

Me	Run No.	Melt concn (atom% *M*)	Solid solution concn (atom% *M*)	Precipitate phases present	*M*–B dist. (Å)
Ca	193	1.5	≤0.02	CaB_6	2.86
Mo	62	1.0	0.3	MoB_4, Mo_2B_5	2.35
Ru	46	1.0	0.05	RuB_2	2.24
W	200	1.0	0.3	WB_4	2.35
Ir	48	2.0	0.06	Ir_3B_4	2.16

unambiguously decide which model is correct.

1. Ca. We prepared samples of β-boron from the melt with a nominal composition of 1.5 atom% Ca. The electron-beam microprobe studies showed that the Ca solubility in β-boron is ≤0.02 atom% (see Table X). This is for β-boron in equilibrium with a CaB_6 precipitate phase, which did appear with about the expected concentration. It has been reported (*27*) that 1 atom% Ca alters the electrical properties of hot-pressed, polycrystalline β-boron. From the present data we suspect that this effect may be due to CaB_6 inclusions. In the present series no single-crystal X-ray studies were made on Ca-doped β-boron.

2. Sc. Scandium in β-boron has been studied (*1*) at a doping level of 3.4 atom%. Combining the present results with this previous study we conclude that the occupied dopant positions are those given in Tables IIIb and VIII. Our results show that at the 1.5 atom% level the E site is the main one that is occupied and that the substitution for pairs of boron B4 atoms is nonexistent. We find that in undoped β-boron as well as in samples Sc180 and Sc192 there is extra electron density at the center of the B4–B4 bond. The peak height corresponds to approximately 0.4 e/Å^3 both in pure, undoped boron and in Sc180. In sample Sc192 this peak rises to 0.63 e/Å^3, while the peak midway between B6 and B8 rises to 0.61 e/Å^3 from its value of 0.49 e/Å^3 in pure boron. There is a small increase in the electron density as Sc is added. In Sc192 this could be interpreted as a $P \simeq 0.2\%$ occupancy by Sc atoms at the center of the B4–B4 bond. We believe that Sc atoms do not replace B4–B4 pairs in any of our samples, i.e., no Sc(4) atoms are found. What happens is that electrons donated to the boron framework by the Sc collect there.

In studying Sc192 we used 1062 independent reflections while Callmer (*1*) used only 1031. Callmer's *R* value was 4.7%; ours was 5.1%. Our *R* value did not change when we assumed that Sc(4) occurs and partially replaces some B4 atoms. Thus we suggest that the extra electron density near the center of the B4–B4 bond seen by Callmer is really only electrons. If this supposition is true, then Sc in β-boron does not behave differently than the other transition elements.

3. Ti. No previous studies of Ti positions exist. It is known (*13*) that Ti expands the lattice. Our results show that Ti prefers D sites at the 1.9 atom% doping level. The average Ti–B distances in both the A_1 and D sites are noticeably shorter than for other transition-metal ions. The Ti–B distance in TiB_2 is 2.38 Å in Table VIII. This is considerably larger than the maximum of 2.183 Å for the A_1 site in Fig. 2. Thus we can conjecture that Ti may have lost some electrons on entering the A_1 site. For example Ti^{1+} would have approximately the correct radius (1.1 Å) to fit into an A_1 site. Ti may donate even more than one electron to boron. Note that the Ti–B bond distance has been found to be especially short (2.39 Å) in the compound TiB (*28*).

The other notable feature of Ti106 and Sc192 is the low value of Σ_1; the B17 and B18 sites do appear to be vacant with <3% of a boron atom present in these sites.

4. V. Some vanadium results are given in our previous paper (*2*). At that time the boron sites B17, B18, and B19 were unknown

and were thought to be vacant. However, a reanalysis of the same data with more insight into the actual structure of β-boron has shown that the B17 and B18 sites in samples V66 and V91 are partially occupied (see Table IIIa). As shown in Fig. 3 most of the vanadium occurs in the A_1 sites with a small fraction in the A_2 and D sites. These other sites only become occupied at the higher vanadium concentrations. For sample V66 the vanadium occupancy of the D site, after reanalysis, is $\leq 1.7\%$. Note that vanadium is the only transition metal found in the A_2 site (see Table VIII).

5. Cr. The previous work (*3*) on Cr was for a doping level of 2.4 atom% where Cr entered both A_1 and D sites. Sample Cr93 at 2.0 atom% agrees with the previous results. We find that at concentrations up to 1.5 atom% the Cr enters only the A_1 sites. At the maximum Cr concentration (*3*) the fraction of all the Cr atoms that are in the A_1 sites is 0.57; the other fraction, 0.43, occupies the D sites. Chromium apparently has the best "fit" for the A_1 site of any of the transition elements (see Fig. 3). Vanadium is a close contender.

For Cr115, grown by the slow cooling method, the value of Σ_1 is $99 \pm 3\%$. This indicates that the B17–B18 pairs are nearly at their maximum concentration and the B13 occupancy is near to its minimum value. Samples Cr65 and Cr93, grown by the fast-cooling method, have lower Σ_1 values which suggests that crystal perfection is less easily attained during fast cooling.

6. Mn. A previous study (*4*) at 4.2 atom% Mn showed that Mn occupies A_1, D, and E sites. The present study at 0.73 atom% shows that the A_1 and D sites are occupied in about the same ratio but both with a much greater preference than for the E sites. The fraction of all the dopant atoms that occur in A_1 sites at this lower doping level is 0.128, see Fig. 3. The Mn concentration in the A_1 sites is much lower than that for other transition elements of comparable size. Mn and Cu are similar in this respect. This difference from the other transition metals may be associated with electron transfer effects where half filled or completely filled d shells exhibit special stability.

7. Fe. A previous study (*5*) at 2.0 atom% Fe showed about equal concentrations of Fe in the A_1 and D sites. Our present results show that at the 1.0 atom% concentration the A_1 sites are preferentially filled. Note also the high electron concentration at the center of the B4–B4 bond in Table IX.

8. Co. No previous studies of Co positions have been reported; however, Co is soluble (*13*). We find comparable quantities of Co in A_1 and D sites at 1.5 atom% Co. Sample Co103 is very similar to sample Ni100, and both were slowly cooled. The B17–B18 concentration in Co103, however, is somewhat lower than expected.

9. Ni. A previous study of Ni was reported (*6*) on single crystals. The major difference with the present results is that we do not find Ni(3) and Ni(4) atoms. We find considerable electron density at the positions assigned to Ni(3) and Ni(4). We believe, however, that these represent boron atoms because the bond lengths are consistent with boron–boron bonds, and because B17 and B18 have been found at these positions in undoped β-boron (*23*). Thus Ni(4) is really B17d and Ni(3) is really B18 (see Tables III and IV). Since B17 and B18 occur in undoped β-boron, they may also occur in Ni-doped samples if the D sites are not fully occupied. Such is the case for $NiB_{48.5}$ (*6*) and for the present three different Ni samples.

We also note that for Ni samples in Table III the sum $\Sigma_1 + \Sigma_2$ varies from 107 to 111%. For $NiB_{48.5}$ of Lundström *et al.* (*6*) we calculate this sum to be 101.6(8)% if we convert their Ni(3) and Ni(4) concentrations to the equivalent in boron. An upper bound on $\Sigma_1 + \Sigma_2$ is 100% if none of the D sites are distorted; but, if some of the sites

are Dd, then the upper bound is 117%. All of these results fall within this range.

The Ni-doped samples in Table III show that the distribution of some of the dopant atoms and of some boron atoms is dependent on the cooling rate from the melt. Compare samples Ni135 and Ni71. For the same dopant concentration, the slowly cooled sample, Ni135, shows a much lower occupancy of the A_1 site, distorted B17 positions, and undistorted or D dopant positions. This is a cautionary tale; the details of the crystal structure can depend upon the thermal history of the sample for β-boron. These effects also show up in some of the measured electrical properties (*19*).

10. Cu. Copper has been studied more extensively (*4, 7, 8*) than any other dopant element. In the present study we were interested in slowly cooled samples at low Cu concentrations. We found that these samples at 0.25 and 0.77 atom% Cu showed no copper in the A_1 sites. This is in contrast to Lundström and Tergenius (*8*) who found 30% of the Cu atoms on A_1 sites for quickly cooled, arc-melted samples with 0.23 atom% Cu. Furthermore no other samples (*4, 7, 8*) exhibited such a large fraction of Cu on A_1 sites. We believe that for near-equilibrium conditions Cu prefers first Dd sites, then E sites, and third A_1 sites only if the Cu concentration exceeds 2.0 atom%. It may be that the thermal history of the particular sample plays a role in the Cu distribution just as it did for the Ni-doped samples. There the rapidly cooled sample showed higher concentrations of Ni in A_1 sites.

The E site for Cu in our sample Cu185 had $z = 0.2210$. Thus it is shifted 0.10 Å from the E site found by previous workers (*4, 7*) where $z = 0.2254$.

In Fig. 3 we show the fraction of dopant atoms in A_1 sites. Note that Cu and Mn have much smaller fractions than other transition metals in the first series. This may be an electron transfer effect related to filled (d^{10}Cu) d shells.

From the results in Table II and the literature references (*4, 7, 8*) we see that the maximum fraction of Cu in A_1 sites is most likely about 0.06 while for Ni it is 0.45 under close-to-equilibrium conditions. For further contrast, up to 0.29 of all the Cu can be in E sites while Ni is never found in E sites. Thus two elements adjacent to each other in the periodic table and with very similar radii (see Table VIII) can behave quite differently during incorporation into β-boron.

11. Zr. From Table VIII zirconium is the largest transition element that has high solubility in β-boron. The incorporation of Zr in β-boron has been studied previously by Callmer *et al.* (*9*) on powders. This is the first study on single crystals. We find that a small fraction of the Zr enters the A_1 sites, whereas (*9*) found Zr in only D and E sites. Also in contrast to (*9*) we find an exceptionally high occupation of the B16 site by boron atoms in sample Zr37; it is even higher than in undoped β-boron. This feature is not understood. The sum Σ_1 of 63% is lower for Zr doping than for any other element, but similar to Ti, Sc, and Hf doping. We do not find any evidence for Zr atoms replacing B4–B4 pairs (*9*) (see Table IX).

12. Nb. We have found that at least 0.5 atom% of Nb is soluble in β-boron (see Table II). Studies by Crespo *et al.* (*14*) indicated a very small lattice expansion of a sample saturated with Nb. The present Table Ib is in agreement with this finding. Thus a small lattice expansion does not necessarily mean a very small solid-solubility. The Nb preferentially enters the D sites as shown in Table IIIb, but some enters the A_1 site in a fashion similar to Zr and Ta.

13. Hf. The maximum Hf solid-solubility is at least 1.8 atom%, and our lattice expansion measurements agree with the large lattice expansion found by Crespo *et al.* (*14*). Hafnium prefers the D site at low concen-

trations, but enters E sites and finally A_1 sites at high concentration. It appears to be another example of low Σ_1 values and the exclusion of boron atoms from B17 and B18 sites.

14. Ta. The solid-solubility of Ta is at least 1 atom% from Table II. Just as for Nb the measured lattice expansion found by Crespo *et al.* (*14*) was small, in agreement with our results in Table 1b. The site preferences of D and A_1 sites for Ta are very similar to those for Nb, to which Ta is closely related chemically. No previous studies of the Ta, Nb, or Hf site preferences are known.

15. Mo, Ru, W, and Ir. We have prepared samples of β-boron doped with 1 to 2 atom% of the five elements Ca, Mo, Ru, W, or Ir. The Ca results were discussed earlier. Studies of these five samples with the electron-beam microprobe showed that the solid-solubility was generally low to nonexistent. See Table X for the results. Most of the added metal showed up on the precipitate phases given in Table X and are the phases expected from the known phase diagrams. This low solubility exists despite the fact that the *M*–B distances from known compounds are in the appropriate ranges (except for Ca). No site occupancies were determined for any of these elements. The X-ray lattice parameter results of Crespo *et al.* (*14*) suggest a small, nonzero, solid solubility for Mo, W, and Ir. The solubility of W in β-boron is given by Portnoi *et al.* (*29*) as 0.8 atom%, somewhat higher than the value in Table X.

V. Volume Expansion, Cell Distortion, and Bond Lengths

The results in Tables Ia and Ib show that in general the unit cell volume increases as the dopant content increases. We would like to know whether this volume increase is caused by a uniform lengthening of all of the boron–boron bonds in the structure, or whether certain bonds change while others remain fixed. In pure β-boron there are 20 different boron positions and 61 different bond lengths in the unit cell. Thus a lot of different changes are possible.

The first useful variable is the c_o/a_o ratio of the hexagonal unit cell. The rhombohedral cell angle, α, varies from one doped sample to another by at most 1°. This produces a small variation in c_o/a_o. A convenient measure of the deviation in c_o/a_o is given by:

$$S = \left[1 - \frac{c_o}{2.17978 a_o}\right] \times 10^4. \qquad (9)$$

The c_o/a_o determined by Callmer (*21*) for pure β-boron is $c_o/a_o = 2.17978$ (*11*). A positive value of S corresponds to an increase in α_{rhom} and a decrease in c_o/a_o. Values of S for the present samples from Table Ia and some samples from the literature are given in Table XI. Values of S from Table Ib are more or less consistent with these; note that the undoped samples have values of S close to zero, as would be expected. Table XI shows that both positive and negative values of S occurs, and that the sign of S and its magnitude for the present samples (except for Cu) are generally consistent with the literature. A comparison of Table XI with Table VIII shows that S is positive for A site dopants and negative for D site dopants. At a dopant concentration of about 1 atom% of either one, a value of $|S|$ of ~20 is produced.

If S were always zero, then the added dopants would only produce a uniform volume expansion of the lattice. Clearly this is *not* the case. Thus the length of some bonds must change more than that of others as the various dopants are added.

In Table I we see that the maximum increase in a_o is ~0.6% and in c_o is ~1%. If we look at individual bond lengths we expect that some of them will increase by percentages larger than this because others will hardly change at all [see Eq. (10)]. A

TABLE XI

CELL DISTORTION PARAMETER S FOR METAL DOPANTS IN β-BORON

	Present sample			Literature		
Dopant	Number	Atom% Me	S	Atom% Me	S	Reference
Si				2.7	+41(17)	(*11*)
Ge				1.1	+11(1)	(*12*)
Sc	180	1.24	−29(21)			
Sc	192	1.54	−30(3)	3.4	−77(1)	(*1*)
Ti	106	1.90	−41(8)	Saturated	−29(2)	(*13*)
V	66	0.60	+11(7)			
V	91	1.57	+4(6)	Saturated	+9(2)	(*13*)
Cr	65	1.04	+22(3)			
Cr	115	1.43	+14(6)			
Cr	93	1.48	+33(10)	2.4	+21.2(4)	(*3*)
Mn	67	0.73	−5(8)	4.2	−18(2)	(*4*)
Fe	64	1.12	+18(6)	2.0	+4(2)	(*5*)
Co	103	1.52	+18(6)	Saturated	+8(2)	(*13*)
Ni	135	0.73	+7(7)			
Ni	71	0.88	~0			
Ni	100	1.64	+32(14)	2.0	+16(1)	(*6*)
Cu	130	0.26	+6(7)	4.2	+8(2)	(*7*)
Cu	185	0.77	−13(5)	3.4	+10(1)	(*4*)
Zr	37	0.69	−9(9)	1.9	−58(1)	(*9*)
Nb	162	0.50	−6(2)	Saturated	−9(1)	(*14*)
Hf	174	0.41	−19(6)			
Hf	169	1.96	−46(5)	Saturated	−60(1)	(*14*)
Ta	170	1.03	−20(3)			
Mo				Saturated	+2(1)	(*14*)
W				Saturated	+3(1)	(*14*)

Note. S values from Table Ia.

convenient way to analyze the changes is to first note that the structure of β-boron is built up of various boron units or clusters bonded together at a few contact points (*20, 21*). There are two types of isolated icosahedra labeled I and II. The third unit is a B_{28} cluster made up of three fused icosahedra of type III. Experimentally we find that the internal boron–boron bonds of the icosahedra change very little as dopants are added; however, the bonding distances between clusters do change. The boron–boron bond lengths within the clusters may increase or decrease by as much as ±2% for the larger size dopants at high concentration. However, the values of the average bond length for all 30 bonds within the icosahedra do not change by more than ±½%. This limit of a ±½% change of the average bond length is also true for the published literature on β-boron containing the maximum concentrations of transition metal ions (*1–9*). A theoretical study by Howard *et al.* (*30*) of the expected change in the average bond length of a B_{12} icosahedron when the required two extra electrons are supplied from electron donors predicts a change of −0.44%, i.e., a shrinkage. The accuracy of the present measurements is not sufficient to see such a charge-transfer effect. We conclude that the critical bond lengths to examine are those few bonds between the clusters.

VI. Cluster–Cluster Bonds

The β-boron structure contains boron icosahedra of three types:

I, icosahedron composed of 6B5 + 6B6 atoms;

II, icosahedron composed of 4B1 + 4B2 + 2B7 + 2B9 atoms;

III, icosahedron composed of 2B3 + 2B4 + 1B8 + 1B10 + 2B11 + 2B12 + 1B13 + 1B14.

The weighted average of boron–boron bond distances, L, within these three icosahedra are (*23*):

$$L(\mathrm{I}) = 1.766(5)\ \text{Å}$$

$$L(\mathrm{II}) = 1.840(6)\ \text{Å}$$

$$L(\mathrm{III}) = 1.813(5)\ \text{Å}.$$

The weighting takes account of the fact that some identical bond distances between atoms occur more than once in each icosahedron. The cluster-to-cluster bond lengths are all listed in Table XII. In pure boron the average intercluster bond length is 1.718(8) Å. For example two neighboring Type II icosahedra are joined by a bond between two B1 atoms. For the samples investigated here the range of B1-to-B1 bond distances is 1.875 to 1.991 Å. The difference in length, Δl, between the largest and smallest

TABLE XII

RANGE OF BOND LENGTHS BETWEEN BORON CLUSTERS FOR PRESENT SAMPLES

Bond	Cluster pair	Range of bond lengths (Å)	l_0 (Å)	$\Delta l/l_0$ (%)	Bond tilt w.r.t. c-axis
B1–B1	II–II	1.875 → 1.991	1.880(6)	6.2	90.0
B2–B3	II–III	1.719 → 1.764	1.726(5)	2.6	53.6
B4–B4	III–III	1.669 → 1.689	1.677(5)	1.2	66.2
B5–B7	I–II	1.701 → 1.743	1.728(5)	2.4	37.4
B6–B8	I–III	1.622 → 1.633	1.630(5)	0.7	77.5
B9–B10	II–III	1.697 → 1.728	1.698(5)	1.8	17.3
B13–B15	III–B–III	1.686 → 1.725	1.686(5)	2.3	38.2

is $\Delta l = 0.116$ Å. Dividing this by the bond length, l_0, in pure β-boron gives:

$$\Delta l/l_0 = 6.2\%. \qquad (10)$$

This is the magnitude of Δl expected from the variation seen in a_0 and c_0, and is the largest bond elongation produced in any of the samples in Table I. Smaller values are found for the other bonds in Table XII. Note that $\Delta l/l_0$ increases almost linearly as l_0 increases. The longer bonds are more easily stretched by the presence of dopant atoms or donated electrons.

Those present samples for which the bond length increases are greater than 1.5% of the length, l_0, in pure boron are listed in Table XIII. From this table it can be seen that dopants that primarily occupy the A_1 site produce B1–B1 bond expansion. Since this bond lies in the a–b plane it produces an increase in a_0 but not c_0, and thus yields a positive value of S. The dopants such as Hf that occur predominantly in the D sites produce elongation of the B2–B3 and B13–B15 bonds. These bonds, particularly B13–B15 and B5–B7, are more nearly parallel to the c-axis and produce negative values of S. The Ni dopants act in both ways simultaneously because both A_1 and Dd sites are involved.

The intercluster bond distances are even larger for higher dopant contents. Table XIV gives our results for Hf and some others from the literature (*1–6*) for samples doped with transition metals at the solid-solubility limit. Note that the effects are very similar to those in Table XIII, but are generally slightly larger. Scandium dopants are the only ones that produce a noticeable decrease in an intercluster bond distance, here the B5–B7 bond.

VII. Conclusions

This study of the atomic locations of transition metal dopants in β-boron in-

TABLE XIII

PRESENT SAMPLES WITH INTERCLUSTER BONDS DIFFERING FROM l_0 BY MORE THAN 1.5%

Sample No.	Bond	Bond length (Å)	Diff. (%)	Dominant dopant site	S
Sc192	B1–B1	1.916(10)	+1.9	E	−30(3)
V91	B1–B1	1.935(10)	+2.9	A_1	+4(6)
Cr65	B1–B1	1.964(5)	+4.5	A_1	+22(3)
Cr115	B1–B1	1.991(5)	+5.9	A_1	+14(6)
Cr93	B1–B1	1.974(8)	+5.0	A_1	+33(10)
Ni100	B1–B1	1.928(10)	+2.6	A_1 + Dd	+32(14)
Hf169	B2–B3	1.764(5)	+2.3	D	−46(5)
Sc180	B5–B7	1.701(9)	−1.6	E	−29(21)
Sc192	B5–B7	1.700(9)	−1.6	E	−30(3)
Sc180	B9–B10	1.728(9)	+1.8	E	−29(21)
Sc192	B9–B10	1.732(9)	+2.1	E	−30(3)
Ni71	B13–B15	1.717(10)	+1.8	Dd	~0
Ni100	B13–B15	1.725(9)	+2.3	A_1 + Dd	+32(4)
Hf169	B13–B15	1.721(8)	+2.1	D	−46(6)

Note. S values from Table Ia.

TABLE XIV

PERCENTAGE CHANGES[a] IN THE INTERCLUSTER BOND DISTANCES FOR β-BORON SAMPLES SATURATED WITH TRANSITION METALS AT THE GIVEN CONCENTRATION (DATA FROM LITERATURE EXCEPT FOR Hf)

Bond	Sc	Cr	Mn	Fe	Ni	Cu	Hf169
B1–B1	+2.4%	+4.9%	+3.5%	+1.7%	+2.5%	+1.6%	
B2–B3	+2.0%						+2.3%
B5–B7	−3.1%						
B9–B10	+3.5%		+1.7%				
B13–B15	+1.9%		+1.8%		+2.4%	+1.7%	+2.1%
Atom% metal	3.4%	2.4%	4.2%	2.0%	2.0%	3.4%	2.0%
Reference	(*1*)	(*3*)	(*4*)	(*5*)	(*6*)	(*4*)	

[a] For changes ≥1.5%.

cludes, we believe, all of those with solid-solubilities ≥ 0.5 atom%. We find that these dopants predominantly enter the A_1, D, and E sites, with some vanadium occurring in A_2 sites. No evidence is seen for the substitution of these dopants into boron sites of the icosahedral framework As the dopant concentration is increased, some boron atoms are usually forced out of the sites with low boron percentage occupancies such as B16, B17, B18, B19 and B20. In addition, the percentage occupancy of B13 can be decreased from 76 to about 63%. There is competition between dopant atoms and nonicosahedral boron atoms for space in the structure. For all three sites the doping is neither interstitial nor substitutional; usually some boron atoms are displaced by the dopants. Thus we term this "displacive dopant behavior," and the semiconductor doping is "displacive" doping.

The unit cell volume generally expands as the dopant content increases. The expansion takes place primarily at the intercluster bonds where length changes up to +6% have been seen. For certain bonds and certain dopants an intercluster bond shrinkage is observed, especially for scandium doping where a −3% change is seen.

The exact location of and the distribution of the dopant atoms between several different possible sites is rather dependent on the previous thermal history of the samples. To some extent, size considerations are useful guides, and the small size dopants enter A_1 and A_2 sites, intermediate size ones enter D sites, while the largest enter E sites. The upper limits on the maximum dopant content of the crystal for an element which enters only one site are:

$$A_1 = 1.87 \text{ atom\%}$$

$$D = 2.79 \text{ atom\%}$$

$$E = 1.84 \text{ atom\%}.$$

Because of competition between A_1 and E occupancy the maximum transition metal content is about 4.7 atom%. Manganese doping approaches this at 4.2 atom%.

Acknowledgment

The authors would like to thank W. S. Knapp for growing most of the β-boron samples studied in this report.

References

1. B. CALLMER, *J. Solid State Chem.* **23,** 391 (1978).
2. M. GARBAUSKAS, J. S. KASPER, AND G. A. SLACK, *J. Solid State Chem.* **63,** 424 (1986).
3. S. ANDERSSON AND T. LUNDSTRÖM, *J. Solid State Chem.* **2,** 603 (1970).

4. S. ANDERSSON AND B. CALLMER, *J. Solid State Chem.* **10,** 219 (1974).
5. B. CALLMER AND T. LUNDSTRÖM, *J. Solid State Chem.* **17,** 165 (1976).
6. T. LUNDSTRÖM, L. E. TERGENIUS, AND I. HIGASHI, *Z. Kristallogr.* **167,** 235 (1984).
7. I. HIGASHI, T. SAKURAI, AND T. ATODA, *J. Less-Common Met.* **45,** 283 (1976).
8. T. LUNDSTRÖM AND L. E. TERGENIUS, *J. Less-Common Met.* **47,** 23 (1976).
9. B. CALLMER, L. E. TERGENIUS, AND J. O. THOMAS, *J. Solid State Chem.* **26,** 275 (1978).
10. R. MATTES, L. MAROSI, AND H. NEIDHARD, *J. Less-Common Met.* **20,** 223 (1970).
11. M. VLASSE AND J. C. VIALA, *J. Solid State Chem.* **37,** 181 (1981).
12. T. LUNDSTRÖM AND L. E. TERGENIUS, *J. Less-Common Met.* **82,** 341 (1981).
13. J. O. CARLSSON AND T. LUNDSTRÖM, *J. Less-Common Met.* **22,** 317 (1970).
14. A. J. CRESPO, L. E. TERGENIUS, AND T. LUNDSTRÖM, *J. Less-Common Met.* **77,** 147 (1981).
15. H. WERHEIT, *Festkörperprobleme* **10,** 189 (1970).
16. O. A. GOLIKOVA, *Phys. Status Solidi A* **51,** 11 (1979).
17. H. WERHEIT, K. DEGROOT, W. MALKEMPER, AND T. LUNDSTRÖM, *J. Less-Common Met.* **82,** 163 (1981).
18. J. M. DUSSEAU, J. L. ROBERT, B. ARMAS, AND C. COMBESCURE, *J. Less-Common Met.* **82,** 137 (1981).
19. G. A. SLACK, J. H. ROSOLOWKSI, AND M. L. MILLER, "Nineteenth Intersociety Energy Conversion Engineering Conference," Vol. 4, p. 2244, San Francisco (1984).
20. D. GEIST, R. KLOSS, AND H. FOLLNER, *Acta Crystallogr. Sect. B* **26,** 1800 (1970).
21. B. CALLMER, *Acta Crystallogr. Sect. B* **33,** 1951 (1977).
22. J. L. HOARD, D. B. SULLENGER, C. H. L. KENNARD, AND R. E. HUGHES, *J. Solid State Chem.* **1,** 268 (1970).
23. G. A. SLACK, C. I. HEJNA, M. F. GARBAUSKAS, AND J. S. KASPER, *J. Solid State Chem.* **76,** 40 (1988).
24. J. A. IBERS AND W. C. HAMILTON, Eds., "International Tables for X-Ray Crystallography," Vol. IV, Kynoch Press, Birmingham (1974).
25. R. W. G. WYCKOFF, "Crystal Structures," Vol. 4, p. 521, Wiley, New York (1968).
26. G. A. SLACK, D. W. OLIVER, G. D. BROWER, AND J. D. YOUNG, *J. Phys. Chem. Solids* **38,** 45 (1977).
27. O. A. GOLIKOVA, V. K. ZAITSEV, A. V. PETROV, L. S. STILBANS, AND E. N. TKALENKO, *Fiz. Tekh. Poluprovodn. (Leningrad)* **6,** 1727 (1972) [Sov. Phys. Semicond. *(Engl. Transl.)* **6,** 1483 (1973)].
28. B. F. DECKER AND J. S. KASPER, *Acta Crystallogr.* **7,** 77 (1954).
29. K. I. PORTNOI, V. N. ROMASHOV, YU, V. LEVINSKII, AND I. V. ROMANOVICH, *Poroshk. Metall. (Kiev)* (#5) 75 (1967) [*Sov. Powder Metall. Met. Ceram. (Engl. Transl.)* **6,** 398 (1967)].
30. I. A. HOWARD, C. L. BECKEL, AND D. EMIN, *in* "Boron-Rich Solids" (D. Emin *et al.*, Eds.), Amer. Inst. Phys. Conf. Proc. 140, p. 240, Amer. Inst. Phys., New York (1986).